Morphological Effects on Polymeric Mixed Ionic/Electronic Conductors

Journal:	*Molecular Systems Design & Engineering*
Manuscript ID	ME-REV-11-2018-000093.R1
Article Type:	Review Article
Date Submitted by the Author:	06-Feb-2019
Complete List of Authors:	Onorato, Jonathan; University of Washington, Materials Science & Engineering Luscombe, Christine; University of Washington, Materials Science & Engineering

Design, System, Application

Polymeric materials which can conduct electrons and ions have already seen wide usage in applications ranging from biological sensors that improve electrocardiogram sensitivity to improving the capacity of lithium ion batteries. Their usage has resulted in impressive improvements in performance of these devices; however, understanding is limited about the structure of these polymers as it relates to their performance. This review article seeks to address the connection between the structure that polymer chains adopt in the solid state and the ion and electron transporting properties of said polymers. Specifically, this review addresses three different motifs that are used for generating these polymers: blended polymers, block copolymers, and homopolymers. Each type presents different strengths and weaknesses, and responds to changes in morphologies in different ways. With an improved understanding of the influence of morphological factors on these transport properties, rational selection of processing methods to control the ionic and electronic transport in each material to target its usage in a specific application would be possible. It is the authors' hope that this review will encourage greater study of the relationship between morphology and performance, increasing our understanding and control over ionic and electronic transport.

Molecular Systems Design & Engineering

REVIEW ARTICLE

Morphological Effects on Polymeric Mixed Ionic/Electronic Conductors

Received 00th January 20xx,
Accepted 00th January 20xx

DOI: 10.1039/x0xx00000x

www.rsc.org/

Jonathan W. Onorato,[a] Christine K. Luscombe.*[a,b,c]

Mixed ion/electron conducting polymers have recently seen significant interest from a number of research communities, spanning from biological to mechanical. Their ability to conduct ions and electrons in the same material enables their use in a wide range of electrochemical devices. This functionality can be used to improve performance of more traditional devices or enable completely novel ones. Herein the use of blended polymers, block copolymers, and homopolymers as mixed conducting polymer systems is discussed, with special emphasis on connecting polymer structure and morphology to mixed conduction performance. Following this discussion, the outlook for the future of this field is presented.

1. Introduction

Mixed ionic/electronic conductors (MIECs) are a class of materials with growing interest from the academic community due to their wide variety of potential uses. MIECs are materials that can conduct both electrons and ions, and as such serve a unique functionality for applications in electrochemical devices, such as sensors,[1,2] actuators,[3,4] batteries,[5,6] fuel cells,[7] and organic electrochemical transistors (OECTs).[8,9] MIECs can be fabricated from both ceramics and polymers; however, this work will be focused specifically on polymeric MIECs, and will use the term MIEC to refer only to polymeric MIECs.[10,11]

MIECs come in several distinct architectures. The most common type currently is a blended architecture, where a polymer that possesses electronic conduction is blended with a polymer that possesses ionic conduction.[5,12] Additional architectures include block copolymers,[13,14] and homopolymers.[15] Due to the highly complex phase-behavior of these materials and the difficulty of devising new synthetic methods, the links between morphology and MIEC performance are still poorly understood. However, in order to enable rational design, and long-term gains in MIEC performance, the connection between ionic conduction, electronic conduction, and the adopted morphology must be better understood. This rigorous study is still in its infancy, but some early trends have started to be understood, and will be presented here. To understand MIEC performance, it is important to understand the fundamentals of electronic conduction independently of ionic conduction, and likewise for ionic conduction independent of electronic conduction.

1.1 Electronic Conduction in Conjugated Polymers

Electronic conduction in polymeric materials occurs through the overlap of π-orbitals. In conjugated polymers, there is a continuous pathway of overlapping π -orbitals, allowing for free electron migration along the whole polymer backbone, as shown in figure 1. Interchain charge transfer is possible through a hopping mechanism, allowing electrons to hop from the π-orbitals of adjacent polymer chains. This delocalization results in the generation of a band-gap. By increasing the coplanarity of the conjugated backbone, the range over which atomic orbitals interact is extended, decreasing the size of the bandgap, as shown in Figure 1.[16] Planarity of a polymer backbone is highly important to charge conduction, as it extends the range over which a charge can be conducted before a relatively slow interchain hopping process occurs, increasing the electron mobility.[17]

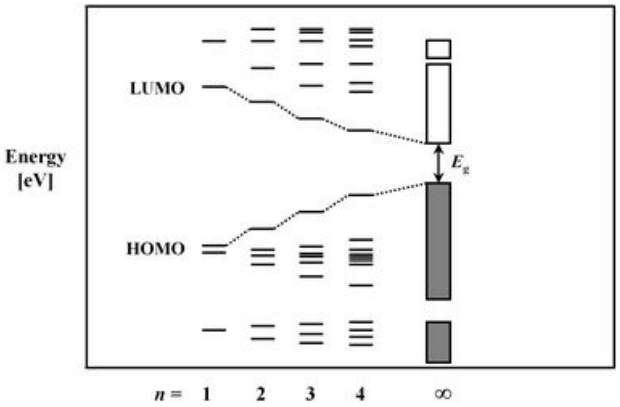

Figure 1: Generation of a band gap with increasing monomers incorporated into a conjugated polymer. Reproduced from Ref. 16 with permission from The Royal Society of Chemistry.

[a] Department of Materials Science and Engineering, University of Washington, Seattle, WA, 98195-2120, USA
[b] Department of Molecular Engineering and Sciences, University of Washington, Seattle, WA, 98195-1652, USA
Department of Chemistry, University of Washington, Seattle, WA, 98195-1700, USA†
*Correspondence should be addressed to Prof. Christine Luscombe, luscombe@uw.edu

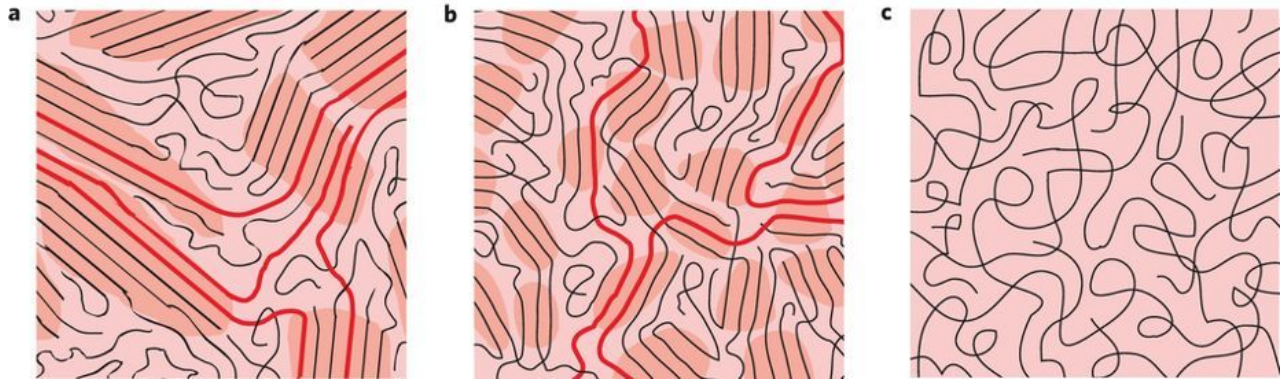

Figure 2: a. Semicrystalline polymer morphology with tie chains highlighted in red. b. Small, disordered aggregates with tie chains highlighted in red. c. Fully amorphous polymer. Figure reproduced with permission from Springer Nature, from Reference 34.

For charges to be transported at bulk, device-level scales, good charge transport must exist in at least two directions. This is because charges must have alternative pathways to travel when defects in the polymer chain or chain ends cause the along-backbone conduction pathway to end. This interchain transport is enabled and improved by the quality of the polymer's π-π stacking. Similar to transport along the backbone, planarizing groups are beneficial as they ease interactions between π-orbitals on adjacent chains. As previously mentioned, this stacking is the basis for crystallite formation in organic electronics, and typically the higher the percentage of crystallinity, the higher the mobility.[18,19] This is due in part to the lack of order in the amorphous regions, resulting in a high percentage of trap states and an increased likelihood of charge recombination.[20,21] Tie-chains are single polymer chains that bridge multiple crystalline domains, providing along-backbone charge conduction between adjacent crystallites. In order for charges to cross amorphous regions, tie-chains are critical, providing improvements in mobility from 10^{-5} to 10^{-2} cm^2/Vs for a commonly studied semiconducting polymer, poly(3-hexylthiophene) [P3HT].[22]

The chemical structure of the polymer repeat unit has a significant impact on the charge mobility. By increasing the length of the solubilizing alkyl side chain from P3HT to poly(3-octylthiophene), a reduction from 1.1 x 10^{-2} to 1.4 x 10^{-4} cm^2/Vs in charge mobility is observed.[23,24] A similar phenomenon is seen with branching chains; introducing an ethyl-branch into a hexyl side chain, poly(3-(2-ethylhexyl)thiophene), reduces the observed field effect mobility by an order of magnitude.[25] Increasing the rigidity of the backbone also increases the mobility, poly(2,5-bis(3-alkylthiophen-2-yl)thieno[3,2-*b*]thiophene) has a charge mobility approximately an order of magnitude higher than P3HT by substituting two thiophene repeat units for a fused thienothiophene unit.[26] Other strategies for improving mobility include synthesizing donor/acceptor copolymers,[27–29] adjusting surface energy levels,[30,31] and increasing regioregularity.[32,33] Most strategies for improving charge transport revolve around rigidifying the polymer backbone and increasing the π-stacking interactions, both features which would be expected to negatively contribute to ionic conduction.[21] However, a recent discovery provides a unique opportunity, showing that high charge mobilities are possible even in highly amorphous materials, if a polymer has a high molecular weight and is sufficiently planar.[34] This is possible because of the connections between local aggregates by the tie chains formed from the long polymer chains, as described in Figure 2. From this, it could be possible to develop a highly open, aggregate-based conjugated polymer that could co-optimize conduction of electrons and ions.

All of the aforementioned techniques focus upon improving charge mobility, however, electronic conduction is dependent upon not only charge mobility, but also the concentration of charge carriers, N, by:

$$\sigma_e = q_e N \mu_e$$

Where σ_e is the conductivity of the charge, q_e is the charge of an electron, and μ_e is the mobility of the charge. The number of charge carriers can be influenced by doping the polymer structure. The small molecule dopant interacts with the polymer backbone, either adding or removing an electron to introduce additional charge carriers into the system.[35] Doping represents an important mechanism of increasing charge conduction in conjugated polymers. This segment represents an extremely brief overview of conductivity in polymers to aide understanding of MIEC conduction properties. Polymer electronic conduction is a rich and nuanced subject, and the interested reader is directed to several excellent reviews on the topic for further details.[36,37]

1.2 Ionic Conduction in Non-conjugated Polymers

Ionic conduction in non-conjugated polymers is a well-studied phenomenon. Contrary to electronic conduction, ionic conduction is improved in less dense structures, in order to accommodate the relatively large size of ionic charge carriers. In a solid-state sample, ions move by random hopping between open adjacent positions in the structure.[38] The nature of the ion has a significant impact on the rate of ion migration; the larger the ion, the slower the motion through the polymer structure,

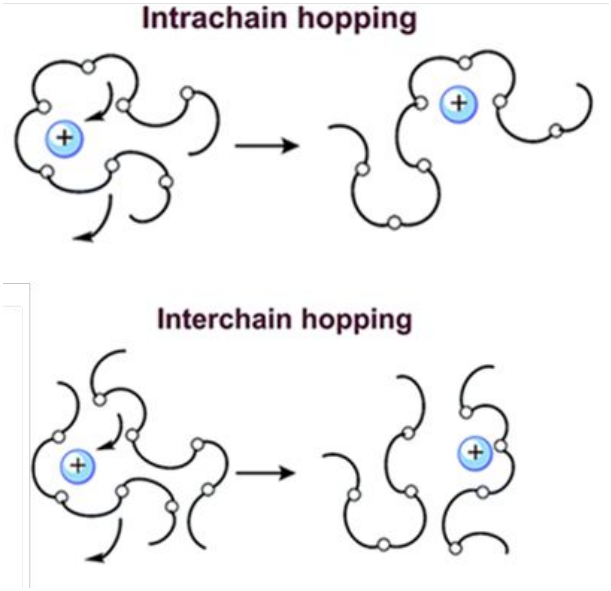

Figure 3: Mechanisms of ionic conduction in solid polymer electrolytes. Figure reproduced by permission of The Royal Society of Chemistry from Reference 38.

and thus the lower the ionic conductivity. This originates from the increased activation energy of the ion hopping between adjacent open sites of a matrix with increasing ionic size, an effect that is due to the increased lattice distortion that has to occur to allow the ion to pass.[39,40]

In addition to the size of the ion, the identity of the salt from which the ion is dissociated is highly important. If the ion pair does not dissociate, it will not respond to an applied voltage, and will not participate in conduction. As such, it is important to choose a counterion that is readily dissociated from the ion of choice. In lithium salts, bulky counterions such as TFSI and PF_6 tend to find use, as they do not readily transport in poly(ethylene oxide) [PEO] structures.[41] The extent of dissociation is also influenced by the dissolution media; incorporating polar, coordinating atoms into the polymer acts to increase the extent of dissociation by stabilizing the charge of the free ion.[41] Typically, atoms like oxygen and nitrogen are used for this purpose, due to the difference in electronegativity between these atoms and carbon. The relatively small size is also advantageous, as it allows a greater density of coordinating groups around an ion, resulting in highly general coordination for ions.[42] The conductivity of the sample is dependent upon this dissociated ion concentration, N_{ion}, through:

$$\sigma_{ion} = N_{ion} q_{ion} \mu_{ion}$$

Where μ_{ion} is ionic mobility, q_{ion} is the charge of the ion, and σ_{ion} is ionic conductivity.

In addition to dissociating ions, the polymer structure plays an important role in the transport of the ionic species. The random hopping of these ionic species is assisted by the reptation, or polymer chain motion, of the coordinating polymer. The reptation of a polymer chain is increased with increasing temperature, so ionic conductivity tends to also increase. This reptation can induce both intrachain and interchain transport of ions. The mechanism for each is shown in Figure 3.[38]

Currently, the prototypical solid-state ionic conductor is PEO. PEO is a particularly attractive ionic conductor, due to several properties arising from its chemical structure. The polymer has a T_g well below room temperature, allowing for ready motion of chains in the amorphous regions.[43] It also has high chain flexibility, allowing coordination of a variety of cations (*e.g.* Na^+, Li^+, Mg^{2+}, K^+, etc.), making it a highly general ion conductor.[42] Unfortunately, PEO also has a strong tendency to crystallize, resulting in poor intrinsic conduction below its melting temperature due to inhibited chain motion.[44,45] To remedy this, several strategies have been used to suppress crystallization, including introducing chain branching,[46,47] adding plasticizing agents,[48,49] and synthesizing brush polymers.[50,51]

While there is evidence that ionic transport in crystalline PEO still occurs, it is unclear if such transport will occur in MIEC crystallites due to the presence of π-π interactions.[35,52] Recent work investigating the effects of doping on conjugated polymer structure indicated that dopant molecules do not enter into the crystalline regions, and instead reside in the amorphous regions of the polymer, due to the increased available free volume.[53,54] It thus remains unclear whether MIECs will demonstrate the same behavior, or will demonstrate crystal intercalation and transport in the crystalline regimes upon introduction of ion coordinating groups.

2. MIECs - Conduction and Morphology

2.1 OECTs

OECTs are often used as a tool for measuring the performance of mixed conductors, as they provide a contained test platform that encompasses both the ionic and electronic elements. During operation of an OECT, a gate voltage is applied across an electrolyte, resulting in the motion of ions into the mixed conductor. This ion migration results in a change in the oxidation state of the mixed conductor, resulting in a measurable difference in current. There are two modes of operation of an MIEC, accumulation and depletion mode. In the case of depletion mode, the MIEC exists in a doped state when unbiased (as in the case of poly(ethylenedioxythiophene):poly(styrene sulfonate) [PEDOT:PSS]). Upon applying a bias, the already present doping ions in the mixed conductor are balanced by the ions migrating into the structure, resulting in a reduction in the extent of doping of the polymer backbone, and a reduction in measured current.[55,56] Alternatively, accumulation mode MIECs exist in an undoped state when unbiased. When a bias is applied, ions migrate into the structure and dope the polymer backbone, resulting in a measurable increase in the current.[9]

Transconductance, or the ratio of the current response from an applied voltage, is a commonly used parameter for organic field-effect transistors (OFETs). In OFETs, the effect is localized to the interface, and as such has only an areal dependence on its magnitude.[57] However, due to the possibility of bulk doping due to ion migration, organic electrochemical transistors

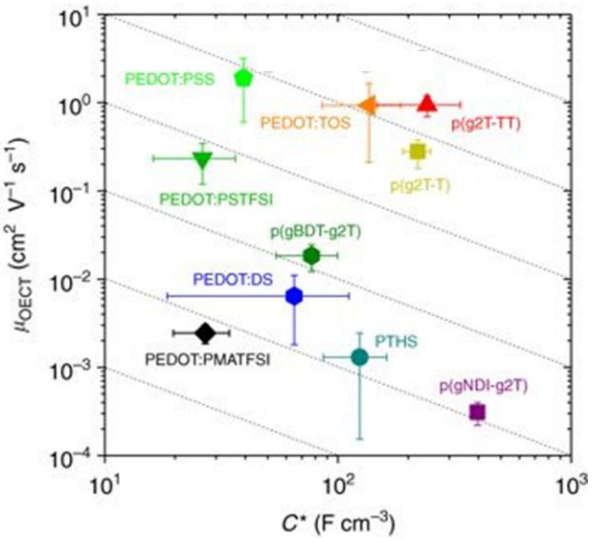

Figure 4: Map of the μC^* figure of merit for several MIEC materials. The dotted lines represent constant values of μC^*. Figure reproduced with permission from Springer Nature from Reference 57.

(OECTs) have a transconductance that is dependent upon the thickness of the film.[58] This changes the equation for calculating transconductance to:

$$g_m = \frac{Wd}{L}\mu C^*(V_{th} - V_G)$$

Where g_m is the transconductance, W is the channel width, d is the thickness of the film, L is the length of the channel, μ is the electronic mobility, C^* is the volumetric capacitance, V_{th} is the threshold voltage, and V_g is the gate voltage.

As device geometry influences the magnitude of transconductance, an alternative metric for comparing MIEC performance, the product of μC^*, has been proposed as a figure of merit for OECTs.[57] μ contains the electronic component, whereas C^* encapsulates the ability of the polymer to uptake and interact with ions, giving a convenient handle on the overall, steady-state performance of the device.[57] As can be seen from the above equation, even polymers with relatively poor electronic mobility can have a high μC^* and thus transconductance with sufficient volumetric capacitance, as shown in Figure 4. However, this figure does not give an indication of the speed of ionic uptake, as these measurements are instead measuring steady-state performance. The interested reader is directed to an excellent review on the physics and history of OECTs, as well as a derivation of a model of OECT device physics.[59,60]

2.2 Applications of MIECs

Herein, only a small sampling of applications will be discussed, and only briefly, in order to give context to the performance and uses of MEICs. In addition to the applications discussed here, MIECs are also used in ion pumps,[61] supercapacitors,[62] gas sensors,[63] electrochromics,[64] thermoelectrics,[65] and actuators.[66]

2.2.1 OECTs

Beyond being used to measure the performance of an MIEC material, OECTs also have several important applications. They have less stringent processing requirements than traditional OFETs, and are able to be made with a variety of different architectures.[67,68] The principle use case of OECTs are for bioelectronics applications. Because OECTs are in direct contact with a liquid during operation, they enable intimate contact with a biological system, which allows for a lower detection threshold for analytes. Due to the volumetric, rather than interfacial, doping process, typically larger transconductance values are produced as compared to OFETs, a feature which enables their use in low-power electronics and is valuable in implanted or long-use devices.[58] OECTs usage in bioelectronics is extensive; three diverse devices are presented herein to give a perspective on their usage. To measure neuronal signals of an epileptic episode in a mouse, an OECT was placed in direct contact with its brain. This configuration resulted in an increased signal-to-noise ratio when compared against existing technologies.[69] An innovative design for low-cost biomarker testing uses the mechanical force generated by a finger pressing on a reservoir to power the pumping of saliva into an OECT-based biological sensor. This PEDOT:PSS-based sensor is able to quantitatively screen for glucose, lactate, and cholesterol levels, with sensitivities in the µM range.[70] A wearable, textile-integrated biosensor has been developed by integrating PEDOT:PSS into a fabric, resulting in a sensor with low power operation that utilizes sweat as the analyte. This system is able to determine the concentration of several biomarkers in sweat, an attractive feature for wearable biosensors.[71]

2.2.2 Battery Binders

Another key use case for MIECs is in batteries, where they see use as electrode binders. MIECs are valuable in this role, as they aid ion motion into and out of the electrode, and facilitate electron extraction all in one material, improving power density and stability over traditional electrode binder mixtures.[5] Introduction of MIECs also helps to mitigate electrode fracturing from the strain generated by the intercalation of lithium; this occurs due to the ductility of the MIEC materials.[72] MIEC incorporation has led to significant increases in longevity and capacity of battery electrodes, especially in newer technologies. For example, an n-type terpolymer based on an alkyl-substituted fluorene copolymerized with fluorenone and methyl benzoate saw increased stability of the silicon electrode, maintaining specific capacities of 2100 mAh/g even after 650 cycles.[73] By introducing a fourth co-monomer, an oligoethylene glycol-substituted fluorene, significant improvements in longevity of silicon electrodes, as well as improvements in cycling rate and capacity were seen. This increase was attributed to the increased polarity given by the oligoethylene glycol side chains.[74] Additionally, investigations into improving the morphology of the binder/electrode mixture have also proven fruitful. A 3-D porous scaffold material made of MIEC polymer with a suspended electrode material saw high rate capabilities, due to the conductive matrix and the porous material enabling greater electrolyte access to the electrode material.[75]

2.2.3 Neuromorphic Computers

Neuromorphic computing is targeting the development of artificial technologies that mimic the functionality of the

neurological system, with the goal of increasing computational efficiency. MIECs are a valuable resource for this technology, as they are able to be manufactured in 3-D architectures, present low power for both operation and switching events, and can be used to generate non-volatile memory states.[76] A target of neuromorphic computing is the memristor, or a transistor that has a "memory" of its past electronic states. PEDOT:PSS-based memristors have been generated with several neuromorphic functions, including short-term depression.[77] Blending PEDOT:PSS with polyethyleneimine (PEI) enables additional functionality, allowing access to 500 distinct electronic states, and switching energies lower than those present for biological systems.[76] Recently, memristor devices have been generated directly using live cells, with a PEDOT:PSS-based memristor being constructed and gated through a *Physarum polycephalum* cell.[78]

2.3 Ion-Specific Effects

Doping in conjugated polymers has seen extensive research since the initial discovery of conduction in polymers; however, this work will focus on those studies which were performed on MIECs. For ionic transport of cations in PEDOT:PSS, the effect of moving down the group 1 period was measured, with the ionic mobility progressing from $H^+ > K^+ > Na^+$.[79] Though K^+ possesses a larger ionic radius, the hydration sphere of Na^+ is significantly larger, and thus, Na^+ transport is slower. It was noted that PEDOT:PSS contained channels that were sufficiently large to transport the bulky choline cation.[79] Investigations into OECT performance with changing cation valence were also performed. OECTs were tested and the sensitivity of the threshold voltage to the different ions were measured in a PEDOT:PSS channel.[80] Unfortunately, the ionic conduction was not directly measured for these systems, and it remains to be seen what effect an increased valency will have on the ionic conductivity in MIECs.

Anions also play an extensive role in ionic conductivity and the extent of polymer doping. In recent work comparing various ions in a P3HT system, it was shown that larger anions, such as PF_6^- and TFSI, resulted in a greater extent of doping when compared against smaller ions, such as ClO_4^- or Cl^-.It was also notable that these larger anions demonstrated a faster rate of ion migration into the polymer structure, along with a lesser degree of hydration.[81] When investigating the same trends in a different mixed conductor, poly(2-(3,3'-bis(2-(2-(2-methoxyethoxy)- ethoxy)ethoxy)-[2,2'-bithiophen]-5-yl)thieno[3,2-b] thiophene) [p(g2T-TT)], a similar trend was observed for the magnitude of g_m, the larger the anion, the larger the g_m. An interesting feature that was also measured was that the larger ions also had a higher solution acidity, which resulted in a lower threshold voltage for the produced OECTs. However, unlike P3HT, it was observed that the larger anions possessed slower doping kinetics.[82] It is interesting that this result appears counter to those seen for P3HT. This difference could be due to the difference in polarity between the mixed conducting polymers, with P3HT being relatively hydrophobic, and p(g2T-TT) hydrophilic.[81,82] There is still need for further clarification of the effects of the anion in mixed conductors, with consideration for the ionic species, the solvent for the ion, and the mixed conducting polymer.

Interactions between ions adjacent to conjugated polymer backbones can have a significant effect on local structure, and can thus influence electronic transport.[83,84] As such, it is important to understand not just electronic or ionic conduction, but the combined transport. The remainder of this review will focus on discussing the connections between MIEC performance and the nanoscale morphology. There are several major types of architectures used to generate MIEC properties in polymeric materials, of which this review will address polymer blends, homopolymers, and block-copolymers.

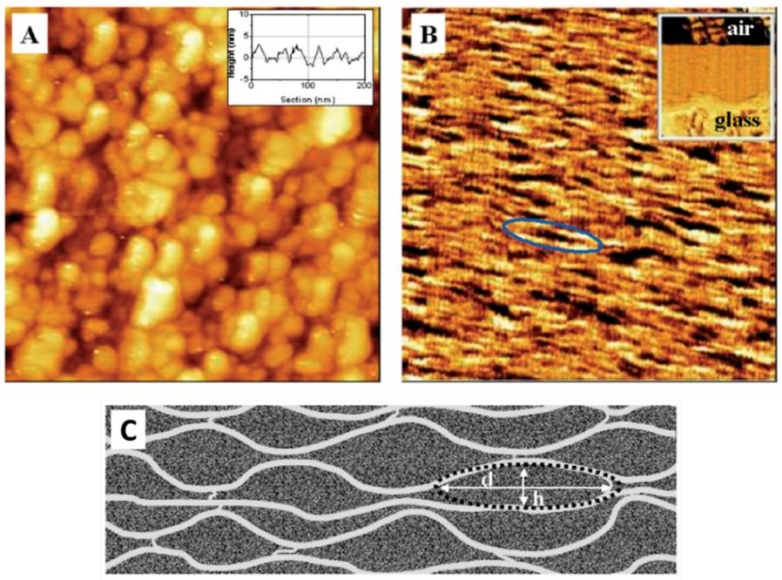

Figure 5: A: Top-down view of PEDOT:PSS spin cast on glass. B: A view of cleaved PEDOT:PSS on glass, with the inset showing the orientation of the sample. C: A schematic representation of the morphology seen, with d indicating the length of PEDOT domains, and h, the height. Figure adapted with permissions from Wiley Publishing Company from Reference 91.

2.4 Polymer Blends

2.4.1 PEDOT:PSS

PEDOT:PSS-based MIECs have dominated research interests in MIECs thus far. PEDOT:PSS is a blended material of poly(ethylenedioxythiophene) and poly(styrene sulfonate), where the sulfonate group of the PSS provides ionic conduction, and the polythiophene backbone of the PEDOT provides electronic conduction.[58,85,86] PEDOT:PSS is available as a commercial suspension in water, and is also readily synthesized and derivatized.[87–89] Additionally, the sulfonate group acts to dope the PEDOT backbone, increasing electronic conductivity of the PEDOT backbone dramatically when compared to neat PEDOT.[60,90] These advantages, along with its excellent film-forming capacity, make PEDOT:PSS an attractive material for MIECs, but predictive relationships remain limited due to its complex morphology. The headway that has been made to understanding the structure-property relationships of PEDOT:PSS MIECs are described below.

PEDOT:PSS adopts a solid-state morphology with PEDOT rich domains separated by a PSS rich matrix; an example of this shown in Figure 5.[91,92] This morphology is generated from the solution state, where PSS anions encapsulate PEDOT-rich domains, solubilizing them in water.[93,94] This skin layer of PSS is maintained after spin-coating, and provides an electrically insulating layer around the PEDOT layer, reducing the overall electronic conduction.[95] In order to improve this conduction, several strategies have been employed, largely revolving around changing or controlling the morphology.

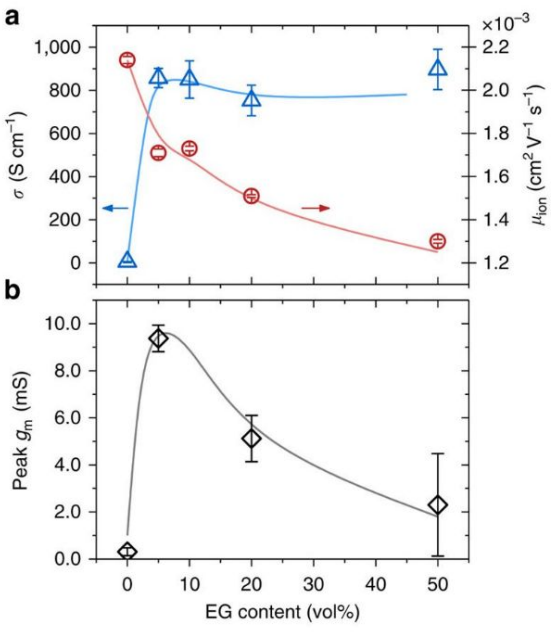

Figure 6: a) The evolution of electronic conductivity and ionic mobility and, b) demonstration of the evolution of transconductance with increasing ethylene glycol content, and thus crystallinity. Figure reproduced with permission from Springer Nature from Reference 95.

One of the primary ways that researchers have worked to change this morphology is by co-processing with a solvent additive. The exact mechanism of enhancement is still unclear, but several theories for the observed electronic conductivity increases have been suggested.[96] One is that these solvents selectively solvate the polar PSS, resulting in a reduction of PSS content in the film.[94,96,97] This reduced PSS content also leads to an increase in the phase purity of the PEDOT domains. This results in a transition from a 1D electronic charge hopping method to a 3D interconnected network for charge transport, resulting in a significant increase in conductivity by as much as three orders of magnitude.[91,98] Another proposed theory is that the introduction of these solvents acts to screen excess PSS from PEDOT, allowing reorienting and better phase-segregation between PEDOT particles.[99] This also results in greater interconnectedness between adjacent PEDOT particles, increasing the electronic conductivity.[99] Processing with a co-solvent can also change the structure of the polymer backbone. For example, with a highly polar co-solvent, the PEDOT chains change from a coil-like structure to an extended coil or even a linear structure.[100,101] This structural change results in better π-stacking interactions between PEDOT chains, enhancing charge transport.[102] Unfortunately, this solvent processing seems to result in a concomitant reduction in ionic conduction, and co-optimization has proven to be difficult. In the case of the ethylene glycol cosolvent treatment, it was observed that with increasing ethylene glycol content, though the electronic conductivity increased, the ionic conductivity decreased. This resulted in an initial increase in transconductance, but then a decrease, as shown in Figure 6.[95]

Post-processing treatment of films with strong acids, such as concentrated sulfuric acid, has also resulted in an exceptionally high electronic conductivity of 4,380 S/cm. This was done through the formation of nanofibrils of PEDOT:PSS, and also through the removal of excess PSS.[103] However, to achieve this extremely high conductivity, more than 70% of the PSS content was removed, likely resulting in extremely poor ionic conduction.[104] Similar experiments using several other acids showed similar, albeit lesser increases in conductivity, but did not show the formation of nanofibrils.[105,106] Instead, similar to changes observed from co-solvent processing, the increases were attributed to a conformational change and a reduction of PSS content.[107,108] While not explicitly measured, it would be reasonable to assume that similar to the co-solvent treatment effects, acid treatment would reduce ionic conduction.

In addition to solvent-based processing, researchers have investigated the effects of introducing cross-linking agents to PEDOT:PSS. In conjugated polymers, introduction of cross-linking agents results in an increase in the density of the structure, and a reduction in the ability of the structure to move.[109] The predominant cross-linking agent for PEDOT:PSS is (3-glycidyloxypropyl)trimethoxysilane (GOPS), which reacts primarily with the sulfonate group of the PSS, as well as with residual hydroxyl groups on substrate surfaces, as shown in Figure 7.[110–112]

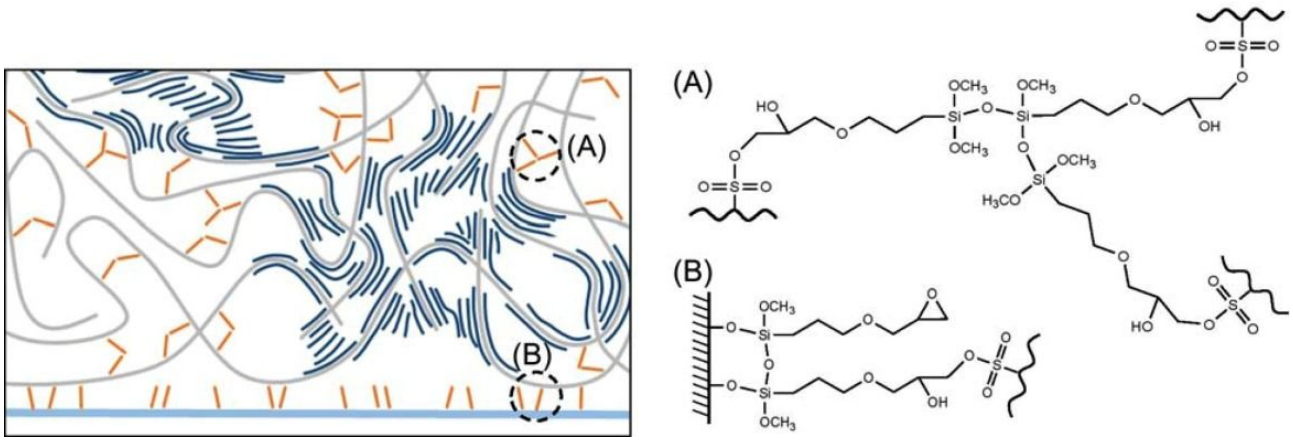

Figure 7: Schematic representation of the morphology and mode of interaction from GOPS treated PEDOT:PSS. Shown at the right are GOPS interactions with A, PSS in the polymer film and B, the substrate. Figure reproduced with permission from Wiley Publishing Group, Reference 115.

While GOPS increases the aqueous stability of PEDOT:PSS based devices, it also reduces both the electronic and ionic conductivity of the sample.[79,113,114] Since GOPS only reacts with the excess PSS, and does not cause a change in the extent of oxidation of the PEDOT, this implies that the reduction in electrical conductivity is only due to a morphological change.[115] The decrease in ionic conductivity was argued to be due to the reduction in swelling of the polymer with water, resulting in a denser polymer structure and reduced space for the ion to be transported through.[79,116,117] The electronic conductivity decrease was proposed to be due to an increase in the degree of separation between conducting PEDOT domains.[115,117] Further work has shown that the degradation of electronic conductivity is proportional to the loading of GOPS, and by tailoring the concentration of GOPS, specific and controllable electronic conduction, as well as aqueous stability, can be obtained.[117] A newer cross-linking agent, divinyl sulfone, demonstrates less of an impact on the electronic conduction, likely due to the difference in cross-linking mechanism, which occurs with residual nucleophiles in the PEDOT:PSS suspension rather than with the PSS.[118] This formulation also presents the interesting advantage of being capable of forming free-standing films with reasonably high stretchability (15% maximum elongation), potentially enabling use as a stretchable, biointerfacing device.[119] Though no morphological studies have been performed, crosslinking with the divalent cation Mg^{2+} through PSS anions results in only a 20% decrease in conductivity as compared to neat PEDOT:PSS, and could present an interesting mode of crosslinking for further study.[120]

In summary, PEDOT:PSS provides a complex morphology that often complicates analysis of the connection between said morphology and its performance. However, it has been shown that treating PEDOT:PSS with solvents results in a significant increase in electronic mobility, but also a significant decrease in ionic conduction due to the increase in phase-segregation and a reduction in overall PSS content. Further, treatment with acid shows the same results, by increasing the degree of order of the PEDOT domains, and by reducing the overall PSS content. Crosslinking presents an interesting way of addressing the lack of stability of PEDOT:PSS in water. By crosslinking, the electronic mobility decreases slightly due to increasing separation between adjacent conducting PEDOT-rich domains. Ionic conduction decreases due to a decrease in the available free PSS, and a reduction in swelling.

2.4.2 Alternative Polymer Blends

While PEDOT:PSS represents an important MIEC blend, several other blended polymers have been investigated to address some of its drawbacks, such as cell toxicity and its high acidity.[121,122] There is not as extensive of literature on other blended polymers; however, efforts, especially into quantifying electronic conductivity, have started appearing. A study into the effects of adjusting the polyelectrolyte in PEDOT:PSS determined several interesting effects. Similarly to PEDOT:PSS, in PEDOT:poly[4-styrenesulfonyl (trifluoromethyl sulfonyl) imide potassium salt] (PSTFSIK) it was observed that there is a relationship between the extent of swelling and the ion conduction of a sample. The greater the extent of swelling, the higher the ionic conduction observed.[123] Unlike PEDOT:PSS, PEDOT:PSTFSIK forms highly interconnected agglomerates upon dispersion from water, which could account for the high electronic conductivity without the need for solvent treatments. PEDOT:PSTFSIK also showed electronic performance enhancement and increased phase purity upon DMSO solvent treatment.[124] Interestingly, increasing the molecular weight of the ionically conducting polymer had a small, negative effect on the overall ionic conductivity, though it also resulted in a small increase in the electronic conductivity.[123] It was noted that counterions for the PEDOT synthesis (K^+ vs. Li^+) have minimal impact on the overall performance of the produced polymer.[123,124] In PEO blends with PEDOT:PSS, with additional PEO content, higher electronic conductivity is seen in the PEDOT phase.[125,126] This was observed to occur through the increased interaction of PSS with PEO, resulting in PEDOT which was better interconnected and more phase pure.[125,127] Encouragingly, this also results in an increase in ionic conductivity.[125,126] Additionally, these

materials demonstrate a high ionic conduction in non-aqueous (acetonitrile) electrolytes, whereas samples with only PEDOT:PSS shows poor ionic conduction, a result likely due to both the partial solubility of PEO in acetonitrile (enabling swelling), and due to the intrinsic conductivity of PEO.[126] This result implies the generality of solvent swelling on ionic conduction, even with intrinsically ionically conducting polymers. An unexpected benefit of blending PEO with PEDOT:PSS is that the material becomes stretchable, able to reach elongations of approximately 35%.[127] In another study, poly[2-methoxy-5-(2-ethylhexyloxy)-1,4-phenylenevinylene] (MEH-PPV) was blended with PEO, and the effects of variations in solvent additives during processing were investigated. The solvent additives were chosen to behave as surfactants, with polar and nonpolar ends, increasing the degree of interaction of the ionic and electronic conductors and resulting in an interpenetrating network of MEH-PPV with PEO, as shown in Figure 8.[128] Similar networks are observed with the blending of MEH-PPV and PEO without surfactants, though the extent of phase-segregation appears to be less.[129] This highly interconnected network is ideal for some MIEC devices, as it allows high mobility of ions and electrons, and ready doping of the conjugated backbone, leading to a strong and quick response to an electrochemical signal.[128,129] It is interesting to note that the introduction of a bifunctional additive appears to significantly improve the lifetime of polymer light-emitting electrochemical cells, likely by stabilizing the interpenetrating network morphology and preventing aggregation.[128] This reduction in degree of phase-separation can also be induced by introducing functionalities into the polymer backbones that improve the compatibility of the ionic and electronic conducting polymers, the domain sizes can be decreased, and the degree of intermixing of the two components improved.[128,130,131]

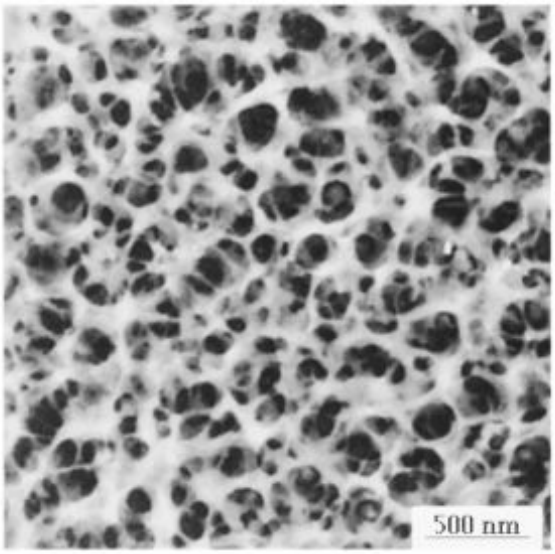

Figure 8: SEM image of an MEH-PPV-b-PEO film cast from a blend containing a surfactant. For this image, the PEO was dissolved out of the material to emphasize the interconnected morphology. Figure reproduced with permission from American Institute of Physics, Reference 128.

There are still many unanswered questions about the relation between morphology and MIEC performance in blended polymer MIECs. However, some initial trends have become clear. It is critical to balance the loading and final quantities of the ionic and electronic conducting components, to ensure that both conduction pathways will be viable. Ionic conduction requires disorder and amorphous structures, whereas electronic requires compact and crystalline.[132] Changing the polyanion for PEDOT synthesis to PSTFSIK results in a morphology with highly interconnected PEDOT domains, which results in a significant increase in conductivity compared to PSS. In polymer blends containing PEO, reducing the size of the domains for each polymer results in better performance of the MIEC by increasing transconductance. Specifically, in blends of PEDOT:PSS with PEO, the PEO acted to increase the purity and ordering of the PEDOT domains, increasing both ionic and electronic conductivity.[125,126] Also, treatment of blends with surfactants could result in a reduction of size scale of phase-segregation, and result in the formation co-continuous interpenetrating networks of ionic and electronic conduction.

2.5 Block Copolymers

Block copolymers (BCPs) can demonstrate phase-segregation between the block phases, a phenomenon which can drive interesting morphological features. This segregation is often generated through hydrophobic/hydrophilic interactions, which is also the case in common block copolymer MIECs; the ion-conducting component is hydrophilic to facilitate interactions with ions, whereas the electron-conducting component is typically hydrophobic. These types of interactions often lead to increased ordering of the respective phases, and, due to the nanoscale length of segregation, results in highly intermixed phases.[133,134] This highly ordered and intermixed morphology seems promising for MIEC performance.

Early work in block copolymers showed that when combined with an insulating block such as polystyrene, P3HT showed self-assembly into nanofibrillar P3HT structures, resulting in an increase in the neat electronic conductivity due to improved ordering of the polymer backbone.[135] The introduction of ionic salts into block copolymers acts to stabilize the phase-separation, increasing the temperature over which BCPs maintain a phase-segregated morphology.[136,137] By replacing the insulating blocks with ionically conducting blocks, additional functionality can be introduced; one such example of this mixed functionality was shown with P3HT-*b*-PEO. The phase-segregation present in this sample, as shown in Figure 9, resulted in an increase in the electronic conductivity in spite of the reduction in P3HT volume fraction, due to the increase in ordering.[13,14]

The lamellar morphology also resulted in bicontinuous pathways for both ionic and electronic conduction, allowing for ionic conductivities of approximately 0.1 mS/cm.[14] By heavily doping the P3HT phase, significant electronic conductivity increases are seen.[138] This result has the added advantage of preventing over-discharging in battery electrodes, as the resistance increases significantly with increasing state of

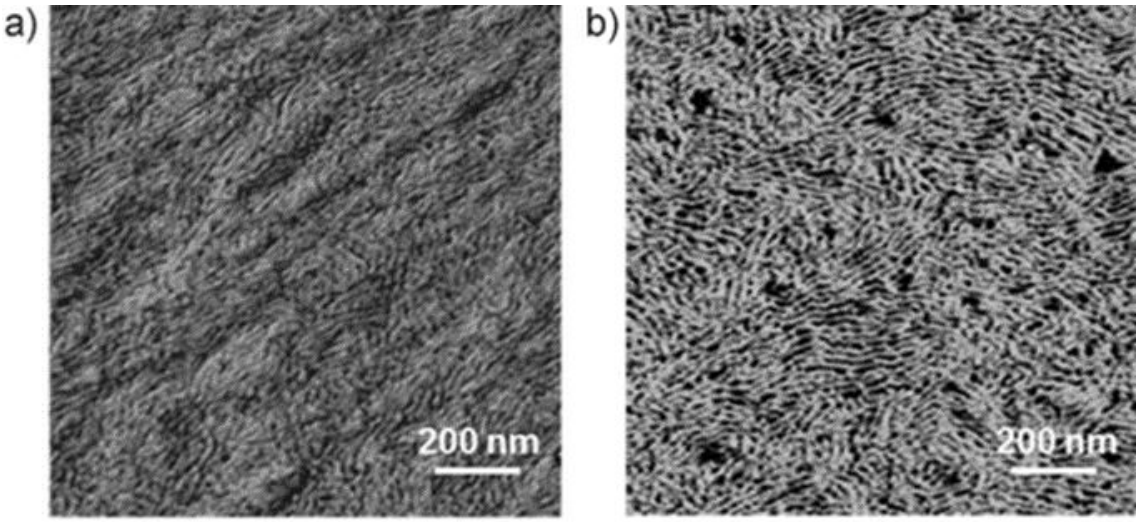

Figure 9:Tapping-mode AFM phase image of a) P3HT homopolymer and b) P3HT-PEO. Figure reproduced with permission from John Wiley and Sons, Reference 14.

discharge due to the reduction in oxidation state. The relative molecular weights of the two blocks also play a significant role. By varying the molecular weight of the components of the block copolymer between 9 kg/mol-2 kg/mol and 5 kg/mol-4 kg/mol P3HT-PEO, the morphology switches from a nanofibrillar to a lamellar phase. This morphological change seems to improve the ionic conduction, though that result could also be due to the increase in PEO weight fraction.[13] It appears that this transition results in a nearly complete exclusion of lithium from the P3HT phase.[13] A reduction of the enhancement of electronic conduction from the addition of PEO is also seen with transition from nanofibrillar to lamellar, though this change could also be due to a reduction in the P3HT content, which has been shown to limit electronic conduction enhancements from phase segregation.[13,14,139]

P3HT-PEO block copolymers present several interesting morphological features that have notable influences on the MIEC performance. Phase-segregation in these materials drives the formation of P3HT nanofibrils in a matrix of PEO, which results in an increased electronic mobility by comparison to neat P3HT. This phase-segregation results in a bi-continuous network of ionically conducting PEO and electronically conducting P3HT with a relatively small degree of separation between the phases due to the chemical bonds between the P3HT and PEO units of the block copolymer. By changing the relative lengths of the P3HT and PEO units, the nanofibrillar morphology can be changed to a lamellar one, a transition which results in an increase in the ionic conductivity. Research into block copolymer MIECs beyond P3HT-*b*-PEO are still quite limited, and currently focus exclusively on morphological characterization, rather than electronic or ionic conduction.[140–142] As such, discussion of these materials has been excluded from this work, though they represent promising potential chemistries, and should be the subject of future research work for MIECs.

2.6 Homopolymers

Some of the earliest work with MIECs involved the investigation of homopolymers such as poly(3-methylthiophene), polycarbazole, and polyacetylene.[143–146] They were poor conductors of ions however, due to the significant hydrophobicity of these polymers.[9] Hydrophobicity results in strong phase-segregation of the ions out of the MIEC matrix and a reduction in the dissociation of the ionic salt, thus reducing both the concentration of ions and the ionic conductivity. Polymers such as polyaniline and polypyrrole saw greater success, due to the increased hydrophilicity of their backbones.[5,147,148] Early work with polyaniline saw difficulties in maintaining consistent morphologies from electrochemical polymerizations, and also incomplete ion-migration into the bulk of the film.[147] Polyaniline and polypyrrole saw significant use as pH sensors, demonstrating marked changes in conductivity.[147,149] An interesting method that resulted in significant increases in electronic conductivity of polyaniline was to gate the material using sulfuric acid, resulting in conductivities as high as 1,000 S/cm. The origination of such a strong increase was proposed to be due to the ability of the weakly bound protons to diffuse through the amorphous regions between highly crystalline islands, effectively mitigating the low conductivity amorphous regions and improving crystalline domain connectivity.[150] In an attempt to mitigate the low ionic conductivity of polypyrrole, a PEO-modified polypyrrole was synthesized, which enabled improved injection of ions into the polypyrrole material, though no discussion as to the morphological basis for this improvement was provided.[151] Recent work using a polymer acid (poly(2-acryl-amido-2-methyl-1-propanesulfonic acid)) as a template has resulted in increased stability, and improved water dispersibility of polypyrrole, which has led to its use in fuel cells and in battery electrodes.[5,7,152]

Polyaniline and polypyrrole both possess significant drawbacks that have limited the scope of their usage. Polypyrrole has an irreversible loss of conduction upon H_2O_2 exposure, and polyaniline loses its conductivity in environments with pH > 5. From these significant drawbacks, and the difficulty of processing polypyrrole and polyaniline, recent research has begun to investigate alternative conjugated backbone chemistries, specifically those conjugated polymers containing hydrophilic moieties to enable improved ionic conduction.

A method for introducing hydrophilic groups is exchanging the typical alkyl side chains of conjugated polymers for oligoethylene glycol chains. As the side chains do not participate in electronic conduction, they can be exchanged without significantly altering the band-gap of the polymer, though they can have a significant influence on the aggregation and crystallization behavior.[25,153,154] Early studies of oligoethylene glycol-modified polythiophene showed that it demonstrated excellent doping stability, an effect attributed to the increased interactions between the hydrophilic side chains and the small-molecule dopants.[155] A study into the effect of either an alkoxy or oligoethylene glycol side chain for a PBTTT backbone showed that, though the morphology of the two was similar, the oligoethylene glycol allowed for bulk ionic transport (which was unfortunately not quantified), whereas the alkoxy did not show any. This could be a result of the intrinsic conductivity of the oligoethylene glycol chains, or it could be a product of swelling. Given results from PEDOT:PSS systems, it seems likely that swelling is a significant component.[79] However, an interesting point was that the volumetric capacitance of the sample was approximately six times larger for this polymer than for PEDOT:PSS. This implies that though ionic conductivity was lower (10% swelling as compared to 155% in PEDOT:PSS), there was a greater availability of electronic doping sites, likely due to the close proximity of ion conducting and electron conducting moieties.[156] If this result proves to be general, it would be a significant advantage for homopolymer MIECs. While an edge-on texture does appear to result in an increase in electronic mobility, it appears to have minimal influence over the ionic conductivity.[157] A more significant influence appears to come from the oligoethylene side chain density. Too high of a density of oligoethylene glycol side chains leads to a reduction in performance, as it is too detrimental to ordering and packing of the π-stack, whereas too low a density results in too dense packing, placing too strong a restriction on ionic transport.[157,158] This modification of conjugated polymers with oligoethylene glycol side chains has also been extended to n-type semiconductors, with a recent paper investigating MIEC performance of an naphthalenediimide (NDI)-based MIEC.[158] The introduction of oligoethylene glycol side chains resulted in a reduction of electronic mobility, a result due to an increase in paracrystalline disorder and a crystalline form transition from 60% Form I and 40% Form II to 90% Form I, reducing π-overlap. Though the comparison is made with different conjugated backbones, increasing the length of the oligoethylene glycol side chains appears to increase the extent of swelling (10% in the PBTTT as compared to 100% in NDI).

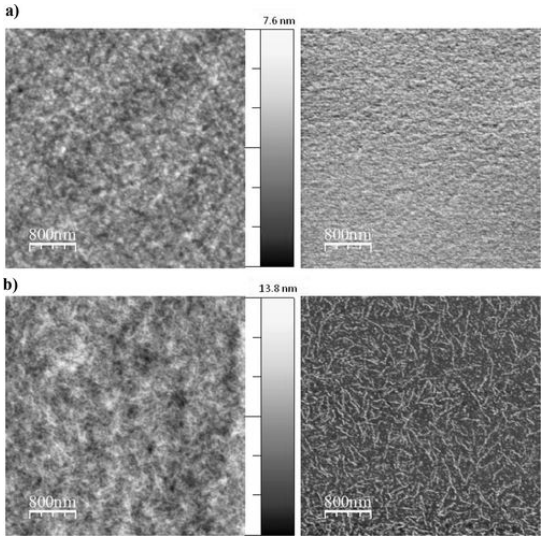

Figure 10: The formation of a nanofibrillar morphology of PTHS upon treatment of the polymer with ethylene glycol. A is the untreated morphology, and B is the treated. Shown to the left is the height, and the right is the phase image for each sample. Figure reproduced with permission from John Wiley and Sons, from Reference 9.

In addition to oligoethylene glycol-substituted conjugated polymers, ionic conductivity can be introduced into conjugated polymers by synthesizing a conjugated polyelectrolyte.[159,160] In one such polymer, poly(3-carboxypentylthiophene), it was shown that the introduction of a polar group, a carboxylic acid, on the terminus of an alkyl side chain was sufficient to enable ionic transport.[161] The effects of solvent treatment with ethylene glycol on another conjugated polyelectrolyte, poly(6-(thiophene-3-yl)hexane-1-sulfonate) tetrabutylammonium [PTHS], were studied. Similarly to PEDOT:PSS, this treatment resulted in increased ordering of the conjugated backbone, resulting in the formation of a fibrillar morphology.[9,99] This results in an increase in electronic conduction, as measured by an approximately sevenfold increase in drain current as compared to pristine PTHS.[9] Contrary to the results in PEDOT:PSS, this treatment actually also increases the swelling of the sample by 20% over the untreated sample and an increase in the ionic conduction, an effect which was attributed to the formation of the fibrillar morphology.[9,95]

There remains significant room for improvement in understanding the connection between morphology and MIEC performance in these homopolymer materials, particularly in understanding the effects of side chain architectures on ionic conduction; however, recent progress has been highly encouraging. Hydrophilicity of at least a component of the system is critical to increasing ion uptake and ionic conductivity. Increasing the availability of electronic sites for doping interactions leads to an increase in volumetric capacitance, an effect which occurs by reducing the distance over which the electronically conducting and ionically conducting segments are separated. The spacing of oligoethylene glycol side chains is critical. At too dense a spacing, the disruptions to the π-stacking ability results in a significant decrease in electronic conductivity, and at too high of a spacing, the crystallite packing becomes too

dense, and there is a reduction in the swelling of the polymer, reducing ionic conductivity. In PTHS, the formation of nanofibrillar structures through ethylene glycol treatment resulted in both an increase in ionic and electronic conductivity, in marked contrast to the results seen in PEDOT:PSS, and an encouraging result, pointing to the possibility that co-optimizing ionic and electronic conductivity is possible.

3. Conclusions and Future Outlook

Herein, the morphological considerations for MIEC performance were discussed for three types of MIEC materials, blended polymers, block copolymers, and homopolymers. Each architecture used for producing MIECs offers its own unique advantages and presents its own challenges. The trends observed for each material class do not necessarily follow between architectures, however, the information gained regarding one system can provide insights into effective methods for other architectures. For example, the treatment of PTHS with ethylene glycol was inspired by the treatment of PEDOT:PSS with ethylene glycol, but the results were not the same for both materials. More work is needed to understand and connect what morphological properties are advantageous for ionic and electronic conduction enhancement, with the ultimate goal to be to develop structure/property relations for each of these architectures of materials.

By summarizing the work that has been done to connect the morphologies generated for each of these architectures to the resultant properties, it is hoped that an expanded appreciation of the importance of this understanding is gained. The consideration of morphology and its influence on MIEC performance is still relatively new, but it presents an opportunity for significant advancement of MIECs and their use in a number of applications. Unexpected results, such as the increasing ionic conductivity with increasing crystallinity in PTHS, should be investigated deeply, then investigated in other polymer systems, for pushing the bounds of our current knowledge. Further investigation into modifying both the length and the polarity of the ion-conducting side chains could prove advantageous. It is currently unclear to what extent changing the length of these chains will modify the ionic and electronic conduction and what effect it will have on the polymer morphology. An additional important consideration is migrating from aqueous electrolytes to organic electrolytes. In particular, it will be interesting to see if the same performance trends observed with aqueous electrolytes are maintained for organic electrolytes, due to the differences in swelling that would be expected for a more non-polar electrolyte. Finally, ionic liquids have proven to be quite powerful in improving the ionic conduction in electrolytes, and incorporation of such moieties into a polymer backbone could result in significant improvements in ionic conductivity, especially when coupled with an ionic liquid as a gating electrolyte. The potential for improvements possible through improved morphological understanding is encouraging and could potentially allow the application of this technology in a host of devices, including such devices as body-integrated sensors and in electrochemical devices such as batteries.

Conflicts of interest

There are no conflicts to declare.

Acknowledgements

The authors would like to acknowledge funding under NSF DMREF Award Number 1629369. This material is based in part upon work supported by the State of Washington through the University of Washington Clean Energy Institute and via funding from the Washington Research Foundation.

References

1 J. E. Zachara, R. Toczyłowska, R. Pokrop, M. Zagórska, A. Dybko and W. Wróblewski, *Sens. Actuators B Chem.*, 2004, **101**, 207–212.
2 A. J. Michalska, C. Appaih-Kusi, L. Y. Heng, S. Walkiewicz and E. A. H. Hall, *Anal. Chem.*, 2004, **76**, 2031–2039.
3 L. Bay, K. West, P. Sommer-Larsen, S. Skaarup and M. Benslimane, *Adv. Mater.*, 2003, **15**, 310–313.
4 H. Stoyanov, M. Kollosche, S. Risse, R. Waché and G. Kofod, *Adv. Mater.*, 2013, **25**, 578–583.
5 Y. Fu and A. Manthiram, *Chem. Mater.*, 2012, **24**, 3081–3087.
6 H. Wu, G. Yu, L. Pan, N. Liu, M. T. McDowell, Z. Bao and Y. Cui, *Nat. Commun.*, 2013, **4**, 1943.
7 A. Murthy and A. Manthiram, *Chem. Commun.*, 2011, **47**, 6882–6884.
8 D. Khodagholy, J. Rivnay, M. Sessolo, M. Gurfinkel, P. Leleux, L. H. Jimison, E. Stavrinidou, T. Herve, S. Sanaur, R. M. Owens and G. G. Malliaras, *Nat. Commun.*, 2013, **4**, 2133.
9 S. Inal, J. Rivnay, P. Leleux, M. Ferro, M. Ramuz, J. C. Brendel, M. M. Schmidt, M. Thelakkat and G. G. Malliaras, *Adv. Mater.*, **26**, 7450–7455.
10 S. Wang, M. Yan, Y. Li, C. Vinado and J. Yang, *J. Power Sources*, 2018, **393**, 75–82.
11 S. Wang, Y. Jiang, Y. Zhang, W. Li, J. Yan and Z. Lu, *Solid State Ion.*, 1999, **120**, 75–84.
12 E. Zeglio, M. M. Schmidt, M. Thelakkat, R. Gabrielsson, N. Solin and O. Inganäs, *Chem. Mater.*, 2017, **29**, 4293–4300.
13 S. N. Patel, A. E. Javier, G. M. Stone, S. A. Mullin and N. P. Balsara, *ACS Nano*, 2012, **6**, 1589–1600.
14 A. E. Javier, S. N. Patel, D. T. Hallinan, V. Srinivasan and N. P. Balsara, *Angew. Chem. Int. Ed.*, 2011, **50**, 9848–9851.
15 C. Deslouis, T. El Moustafid, M. M. Musiani and B. Tribollet, *Electrochimica Acta*, 1996, **41**, 1343–1349.
16 A. Ajayaghosh, *Chem. Soc. Rev.*, 2003, **32**, 181–191.
17 S. Holliday, J. E. Donaghey and I. McCulloch, *Chem. Mater.*, 2014, **26**, 647–663.
18 S. Cho, K. Lee, J. Yuen, G. Wang, D. Moses, A. J. Heeger, M. Surin and R. Lazzaroni, *J. Appl. Phys.*, 2006, **100**, 114503.
19 W. K. Tatum and C. K. Luscombe, *Polym. J.*, 2018, **50**, 659.
20 J.-F. Chang, H. Sirringhaus, M. Giles, M. Heeney and I. McCulloch, *Phys. Rev. B*, 2007, **76**, 205204.
21 A. R. Chew, R. Ghosh, V. Pakhnyuk, J. Onorato, E. C. Davidson, R. A. Segalman, C. K. Luscombe, F. C. Spano and A. Salleo, *Adv. Funct. Mater.*, 2018, **28**, 1804142.

22 K. Gu, C. R. Snyder, J. Onorato, C. K. Luscombe, A. W. Bosse and Y.-L. Loo, *ACS Macro Lett.*, 2018, **7**, 1333–1338.
23 K. Kaneto, W. Y. Lim, W. Takashima, T. Endo and M. Rikukawa, *Jpn. J. Appl. Phys.*, 2000, **39**, L872.
24 S. Savagatrup, A. D. Printz, H. Wu, K. M. Rajan, E. J. Sawyer, A. V. Zaretski, C. J. Bettinger and D. J. Lipomi, *Synth. Met.*, 2015, **203**, 208–214.
25 V. Ho, B. W. Boudouris and R. A. Segalman, *Macromolecules*, 2010, **43**, 7895–7899.
26 I. McCulloch, M. Heeney, C. Bailey, K. Genevicius, I. MacDonald, M. Shkunov, D. Sparrowe, S. Tierney, R. Wagner, W. Zhang, M. L. Chabinyc, R. J. Kline, M. D. McGehee and M. F. Toney, *Nat. Mater.*, 2006, **5**, 328–333.
27 D.-H. Lim, S.-Y. Jang, M. Kang, S. Lee, Y.-A. Kim, Y.-J. Heo, M.-H. Lee and D.-Y. Kim, *J. Mater. Chem. C*, 2017, **5**, 10126–10132.
28 Y. Li, W. K. Tatum, J. W. Onorato, Y. Zhang and C. K. Luscombe, *Macromolecules*, 2018, **51**, 6352–6358.
29 Y. Li, W. K. Tatum, J. W. Onorato, S. D. Barajas, Y. Y. Yang and C. K. Luscombe, *Polym. Chem.*, 2017, **8**, 5185–5193.
30 A. Salleo, M. L. Chabinyc, M. S. Yang and R. A. Street, *Appl. Phys. Lett.*, 2002, **81**, 4383–4385.
31 R. J. Kline, M. D. McGehee and M. F. Toney, *Nat. Mater.*, 2006, **5**, 222–228.
32 J.-S. Kim, J.-H. Kim, W. Lee, H. Yu, H. J. Kim, I. Song, M. Shin, J. H. Oh, U. Jeong, T.-S. Kim and B. J. Kim, *Macromolecules*, 2015, **48**, 4339–4346.
33 R. Mauer, M. Kastler and F. Laquai, *Adv. Funct. Mater.*, 2010, **20**, 2085–2092.
34 R. Noriega, J. Rivnay, K. Vandewal, F. P. V. Koch, N. Stingelin, P. Smith, M. F. Toney and A. Salleo, *Nat. Mater.*, 2013, **12**, 1038–1044.
35 D. T. Scholes, P. Y. Yee, J. R. Lindemuth, H. Kang, J. Onorato, R. Ghosh, C. K. Luscombe, F. C. Spano, S. H. Tolbert and B. J. Schwartz, *Adv. Funct. Mater.*, 2017, **27**, 1702654.
36 M. Jaiswal and R. Menon, *Polym. Int.*, 2006, **55**, 1371–1384.
37 A. Salleo, R. J. Kline, D. M. DeLongchamp and M. L. Chabinyc, *Adv. Mater.*, 2010, **22**, 3812–3838.
38 Z. Xue, D. He and X. Xie, *J. Mater. Chem. A*, 2015, **3**, 19218–19253.
39 P. P. Kumar and S. Yashonath, *J. Chem. Sci.*, 2006, **118**, 135–154.
40 D. B. Shah, K. R. Olson, A. Karny, S. J. Mecham, J. M. DeSimone and N. P. Balsara, *J. Electrochem. Soc.*, 2017, **164**, A3511–A3517.
41 R. C. Agrawal and G. P. Pandey, *J. Phys. Appl. Phys.*, 2008, **41**, 223001.
42 S. B. Aziz, T. J. Woo, M. F. Z. Kadir and H. M. Ahmed, *J. Sci. Adv. Mater. Devices*, 2018, **3**, 1–17.
43 D. Golodnitsky, E. Strauss, E. Peled and S. Greenbaum, *J. Electrochem. Soc.*, 2015, **162**, A2551–A2566.
44 S. Cheng, D. M. Smith and C. Y. Li, *Macromolecules*, 2014, **47**, 3978–3986.
45 J. Siva Kumar, A. R. Subrahmanyam, M. Jaipal Reddy and U. V. Subba Rao, *Mater. Lett.*, 2006, **60**, 3346–3349.
46 M. Watanabe, S. Nagano, K. Sanui and N. Ogata, *Solid State Ion.*, 1986, **18–19**, 338–342.
47 I. Albinsson, B. -E. Mellander and J. R. Stevens, *J. Chem. Phys.*, 1992, **96**, 681–690.
48 C. W. Walker and M. Salomon, *J. Electrochem. Soc.*, 1993, **140**, 3409–3412.
49 S. Das and A. Ghosh, *Electrochimica Acta*, 2015, **171**, 59–65.
50 Z. Wei, S. Chen, J. Wang, Z. Wang, Z. Zhang, X. Yao, Y. Deng and X. Xu, *J. Mater. Chem. A*, 2018, **6**, 13438–13447.
51 L. Qi, Y. Lin, X. Jing and F. Wang, *Solid State Ion.*, 2001, **139**, 293–301.
52 Y. Gao, B. Hu, Y. Yao and Q. Chen, *Chem. – Eur. J.*, 2011, **17**, 8941–8946.
53 R. Giridharagopal, L. Q. Flagg, J. S. Harrison, M. E. Ziffer, J. Onorato, C. K. Luscombe and D. S. Ginger, *Nat. Mater.*, 2017, **16**, 737–742.
54 R. Ghosh, A. R. Chew, J. Onorato, V. Pakhnyuk, C. K. Luscombe, A. Salleo and F. C. Spano, *J. Phys. Chem. C*, 2018, **122**, 18048–18060.
55 A. Savva, S. Wustoni and S. Inal, *J. Mater. Chem. C*, 2018, **6**, 12023–12030.
56 K. Tybrandt, I. V. Zozoulenko and M. Berggren, *Sci. Adv.*, 2017, **3**, eaao3659.
57 S. Inal, G. G. Malliaras and J. Rivnay, *Nat. Commun.*, 2017, **8**, 1767.
58 J. Rivnay, P. Leleux, M. Ferro, M. Sessolo, A. Williamson, D. A. Koutsouras, D. Khodagholy, M. Ramuz, X. Strakosas, R. M. Owens, C. Benar, J.-M. Badier, C. Bernard and G. G. Malliaras, *Sci. Adv.*, 2015, **1**, e1400251.
59 J. Rivnay, S. Inal, A. Salleo, R. M. Owens, M. Berggren and G. G. Malliaras, *Nat. Rev. Mater.*, 2018, **3**, 17086.
60 D. A. Bernards and G. G. Malliaras, *Adv. Funct. Mater.*, 2007, **17**, 3538–3544.
61 N. Abdullayeva and M. Sankir, *Materials*, 2017, **10**, 586.
62 J. Edberg, O. Inganäs, I. Engquist and M. Berggren, *J. Mater. Chem. A*, 2018, **6**, 145–152.
63 S. Virji, J. Huang, R. B. Kaner and B. H. Weiller, *Nano Lett.*, 2004, **4**, 491–496.
64 N. C. Davy, M. Sezen-Edmonds, J. Gao, X. Lin, A. Liu, N. Yao, A. Kahn and Y.-L. Loo, *Nat. Energy*, 2017, **2**, 17104.
65 W. B. Chang, H. Fang, J. Liu, C. M. Evans, B. Russ, B. C. Popere, S. N. Patel, M. L. Chabinyc and R. A. Segalman, *ACS Macro Lett.*, 2016, **5**, 455–459.
66 S. Hara, T. Zama, W. Takashima and K. Kaneto, *Synth. Met.*, 2006, **156**, 351–355.
67 P. Andersson, D. Nilsson, P.-O. Svensson, M. Chen, A. Malmström, T. Remonen, T. Kugler and M. Berggren, *Adv. Mater.*, 2002, **14**, 1460–1464.
68 E. Stavrinidou, R. Gabrielsson, E. Gomez, X. Crispin, O. Nilsson, D. T. Simon and M. Berggren, *Sci. Adv.*, 2015, **1**, e1501136.
69 D. Khodagholy, T. Doublet, P. Quilichini, M. Gurfinkel, P. Leleux, A. Ghestem, E. Ismailova, T. Hervé, S. Sanaur, C. Bernard and G. G. Malliaras, *Nat. Commun.*, 2013, **4**, 1575.
70 A.-M. Pappa, V. F. Curto, M. Braendlein, X. Strakosas, M. J. Donahue, M. Fiocchi, G. G. Malliaras and R. M. Owens, *Adv. Healthc. Mater.*, 2016, **5**, 2295–2302.
71 I. Gualandi, M. Marzocchi, A. Achilli, D. Cavedale, A. Bonfiglio and B. Fraboni, *Sci. Rep.*, 2016, **6**, 33637.
72 S.-J. Park, H. Zhao, G. Ai, C. Wang, X. Song, N. Yuca, V. S. Battaglia, W. Yang and G. Liu, *J. Am. Chem. Soc.*, 2015, **137**, 2565–2571.
73 G. Liu, S. Xun, N. Vukmirovic, X. Song, P. Olalde-Velasco, H. Zheng, V. S. Battaglia, L. Wang and W. Yang, *Adv. Mater.*, 2011, **23**, 4679–4683.
74 M. Wu, X. Xiao, N. Vukmirovic, S. Xun, P. K. Das, X. Song, P. Olalde-Velasco, D. Wang, A. Z. Weber, L.-W. Wang, V. S. Battaglia, W. Yang and G. Liu, *J. Am. Chem. Soc.*, 2013, **135**, 12048–12056.

75 Y. Shi, X. Zhou, J. Zhang, A. M. Bruck, A. C. Bond, A. C. Marschilok, K. J. Takeuchi, E. S. Takeuchi and G. Yu, *Nano Lett.*, 2017, **17**, 1906–1914.
76 Y. van de Burgt, E. Lubberman, E. J. Fuller, S. T. Keene, G. C. Faria, S. Agarwal, M. J. Marinella, A. Alec Talin and A. Salleo, *Nat. Mater.*, 2017, **16**, 414–418.
77 P. Gkoupidenis, N. Schaefer, B. Garlan and G. G. Malliaras, *Adv. Mater.*, 2015, **27**, 7176–7180.
78 G. Tarabella, P. D'Angelo, A. Cifarelli, A. Dimonte, A. Romeo, T. Berzina, V. Erokhin and S. Iannotta, *Chem. Sci.*, 2015, **6**, 2859–2868.
79 E. Stavrinidou, P. Leleux, H. Rajaona, D. Khodagholy, J. Rivnay, M. Lindau, S. Sanaur and G. G. Malliaras, *Adv. Mater.*, 2013, **25**, 4488–4493.
80 P. Lin, F. Yan and H. L. W. Chan, *ACS Appl. Mater. Interfaces*, 2010, **2**, 1637–1641.
81 L. Q. Flagg, R. Giridharagopal, J. Guo and D. S. Ginger, *Chem. Mater.*, 2018, **30**, 5380–5389.
82 C. Cendra, A. Giovannitti, A. Savva, V. Venkatraman, I. McCulloch, A. Salleo, S. Inal and J. Rivnay, *Adv. Funct. Mater.*, DOI:10.1002/adfm.201807034.
83 M. J. Marsella and T. M. Swager, *J. Am. Chem. Soc.*, 1993, **115**, 12214–12215.
84 D. Khodagholy, M. Gurfinkel, E. Stavrinidou, P. Leleux, T. Herve, S. Sanaur and G. G. Malliaras, *Appl. Phys. Lett.*, 2011, **99**, 163304.
85 A. Elschner and W. Lövenich, *MRS Bull.*, 2011, **36**, 794–798.
86 K. Tybrandt, R. Forchheimer and M. Berggren, *Nat. Commun.*, 2012, **3**, 871.
87 S. C. NG, H. S. O. CHAN and W.-L. YU, *J. Mater. Sci. Lett.*, 1997, **16**, 809–811.
88 C. Wang, J. L. Schindler, C. R. Kannewurf and M. G. Kanatzidis, *Chem. Mater.*, 1995, **7**, 58–68.
89 F. Jonas, W. Krafft and B. Muys, *Macromol. Symp.*, 1995, **100**, 169–173.
90 A. Elschner, S. Kirchmeyer, W. Lovenich, U. Merker and K. Reuter, *PEDOT: Principles and Applications of an Intrinsically Conductive Polymer*, CRC Press, 2010.
91 A. M. Nardes, M. Kemerink, R. a. J. Janssen, J. a. M. Bastiaansen, N. M. M. Kiggen, B. M. W. Langeveld, A. J. J. M. van Breemen and M. M. de Kok, *Adv. Mater.*, 2007, **19**, 1196–1200.
92 U. Lang, E. Müller, N. Naujoks and J. Dual, *Adv. Funct. Mater.*, 2009, **19**, 1215–1220.
93 T. Takano, H. Masunaga, A. Fujiwara, H. Okuzaki and T. Sasaki, *Macromolecules*, 2012, **45**, 3859–3865.
94 Y. H. Kim, C. Sachse, M. L. Machala, C. May, L. Müller-Meskamp and K. Leo, *Adv. Funct. Mater.*, 2011, **21**, 1076–1081.
95 J. Rivnay, S. Inal, B. A. Collins, M. Sessolo, E. Stavrinidou, X. Strakosas, C. Tassone, D. M. Delongchamp and G. G. Malliaras, *Nat. Commun.*, 2016, **7**, 11287.
96 S. Zhang, P. Kumar, A. S. Nouas, L. Fontaine, H. Tang and F. Cicoira, *APL Mater.*, 2014, **3**, 014911.
97 S. K. M. Jönsson, J. Birgerson, X. Crispin, G. Greczynski, W. Osikowicz, A. W. Denier van der Gon, W. R. Salaneck and M. Fahlman, *Synth. Met.*, 2003, **139**, 1–10.
98 J. Huang, P. F. Miller, J. S. Wilson, A. J. de Mello, J. C. de Mello and D. D. C. Bradley, *Adv. Funct. Mater.*, 2005, **15**, 290–296.
99 D. A. Mengistie, P.-C. Wang and C.-W. Chu, *J. Mater. Chem. A*, 2013, **1**, 9907–9915.
100 C. M. Palumbiny, C. Heller, C. J. Schaffer, V. Körstgens, G. Santoro, S. V. Roth and P. Müller-Buschbaum, *J. Phys. Chem. C*, 2014, **118**, 13598–13606.
101 J. Ouyang, C.-W. Chu, F.-C. Chen, Q. Xu and Y. Yang, *Adv. Funct. Mater.*, 2005, **15**, 203–208.
102 J. Ouyang, Q. Xu, C.-W. Chu, Y. Yang, G. Li and J. Shinar, *Polymer*, 2004, **45**, 8443–8450.
103 Y. Xia, K. Sun and J. Ouyang, *Adv. Mater.*, 2012, **24**, 2436–2440.
104 N. Kim, S. Kee, S. H. Lee, B. H. Lee, Y. H. Kahng, Y.-R. Jo, B.-J. Kim and K. Lee, *Adv. Mater.*, 2014, **26**, 2268–2272.
105 W. Meng, R. Ge, Z. Li, J. Tong, T. Liu, Q. Zhao, S. Xiong, F. Jiang, L. Mao and Y. Zhou, *ACS Appl. Mater. Interfaces*, 2015, **7**, 14089–14094.
106 D. A. Mengistie, M. A. Ibrahem, P.-C. Wang and C.-W. Chu, *ACS Appl. Mater. Interfaces*, 2014, **6**, 2292–2299.
107 Y. Xia and J. Ouyang, *ACS Appl. Mater. Interfaces*, 2010, **2**, 474–483.
108 A. K. Sarker, J. Kim, B.-H. Wee, H.-J. Song, Y. Lee, J.-D. Hong and C. Lee, *RSC Adv.*, 2015, **5**, 52019–52025.
109 L. Derue, O. Dautel, A. Tournebize, M. Drees, H. Pan, S. Berthumeyrie, B. Pavageau, E. Cloutet, S. Chambon, L. Hirsch, A. Rivaton, P. Hudhomme, A. Facchetti and G. Wantz, *Adv. Mater.*, 2014, **26**, 5831–5838.
110 O. Berezhetska, B. Liberelle, G. D. Crescenzo and F. Cicoira, *J. Mater. Chem. B*, 2015, **3**, 5087–5094.
111 D. Khodagholy, T. Doublet, M. Gurfinkel, P. Quilichini, E. Ismailova, P. Leleux, T. Herve, S. Sanaur, C. Bernard and G. G. Malliaras, *Adv. Mater.*, 2011, **23**, H268–H272.
112 A. K. Y. Wong and U. J. Krull, *Anal. Bioanal. Chem.*, 2005, **383**, 187–200.
113 L. Kergoat, B. Piro, D. T. Simon, M.-C. Pham, V. Noël and M. Berggren, *Adv. Mater.*, 2014, **26**, 5658–5664.
114 R. Colucci, M. H. Quadros, F. H. Feres, F. B. Maia, F. S. de Vicente, G. C. Faria, L. F. Santos and G. Gozzi, *Synth. Met.*, 2018, **241**, 47–53.
115 A. Håkansson, S. Han, S. Wang, J. Lu, S. Braun, M. Fahlman, M. Berggren, X. Crispin and S. Fabiano, *J. Polym. Sci. Part B Polym. Phys.*, 2017, **55**, 814–820.
116 S.-M. Kim, C.-H. Kim, Y. Kim, N. Kim, W.-J. Lee, E.-H. Lee, D. Kim, S. Park, K. Lee, J. Rivnay and M.-H. Yoon, *Nat. Commun.*, 2018, **9**, 3858.
117 M. ElMahmoudy, S. Inal, A. Charrier, I. Uguz, G. G. Malliaras and S. Sanaur, *Macromol. Mater. Eng.*, 2017, **302**, 1600497.
118 D. Mantione, I. del Agua, W. Schaafsma, M. ElMahmoudy, I. Uguz, A. Sanchez-Sanchez, H. Sardon, B. Castro, G. G. Malliaras and D. Mecerreyes, *ACS Appl. Mater. Interfaces*, 2017, **9**, 18254–18262.
119 I. del Agua, D. Mantione, U. Ismailov, A. Sanchez-Sanchez, N. Aramburu, G. G. Malliaras, D. Mecerreyes and E. Ismailova, *Adv. Mater. Technol.*, 2018, **3**, 1700322.
120 L. Yan, X. Gao, J. Palathinkal Thomas, J. Ngai, H. Altounian, K. Tong Leung, Y. Meng and Y. Li, *Sustain. Energy Fuels*, 2018, **2**, 1574–1581.
121 D. G. Harman, R. Gorkin, L. Stevens, B. Thompson, K. Wagner, B. Weng, J. H. Y. Chung, M. in het Panhuis and G. G. Wallace, *Acta Biomater.*, 2015, **14**, 33–42.
122 Y. Zhang, L. Chen, X. Hu, L. Zhang and Y. Chen, *Sci. Rep.*, 2015, **5**, 12839.
123 S. Inal, J. Rivnay, A. I. Hofmann, I. Uguz, M. Mumtaz, D. Katsigiannopoulos, C. Brochon, E. Cloutet, G. Hadziioannou

and G. G. Malliaras, *J. Polym. Sci. Part B Polym. Phys.*, 2016, **54**, 147–151.
124 A. I. Hofmann, W. T. T. Smaal, M. Mumtaz, D. Katsigiannopoulos, C. Brochon, F. Schütze, O. R. Hild, E. Cloutet and G. Hadziioannou, *Angew. Chem. Int. Ed.*, 2015, **54**, 8506–8510.
125 M. B. McDonald and P. T. Hammond, *ACS Appl. Mater. Interfaces*, 2018, **10**, 15681–15690.
126 S. Ghosh and O. Inganäs, *Electrochem. Solid-State Lett.*, 2000, **3**, 213–215.
127 P. Li, K. Sun and J. Ouyang, *ACS Appl. Mater. Interfaces*, 2015, **7**, 18415–18423.
128 Y. Cao, G. Yu, A. J. Heeger and C. Y. Yang, *Appl. Phys. Lett.*, 1996, **68**, 3218–3220.
129 F.-C. Chen, Q. Xu and Y. Yang, *Appl. Phys. Lett.*, 2004, **84**, 3181–3183.
130 F. P. Wenzl, P. Pölt, A. Haase, S. Patil, U. Scherf and G. Leising, *Solid State Ion.*, 2005, **176**, 1747–1751.
131 Y. Cao, Q. Pei, M. R. Andersson, G. Yu and A. J. Heeger, *J. Electrochem. Soc.*, 1997, **144**, L317–L320.
132 J. T. Friedlein, J. Rivnay, D. H. Dunlap, I. McCulloch, S. E. Shaheen, R. R. McLeod and G. G. Malliaras, *Appl. Phys. Lett.*, 2017, **111**, 023301.
133 I. Y. Song, J. Kim, M. J. Im, B. J. Moon and T. Park, *Macromolecules*, 2012, **45**, 5058–5068.
134 C. R. Craley, R. Zhang, T. Kowalewski, R. D. McCullough and M. C. Stefan, *Macromol. Rapid Commun.*, 2009, **30**, 11–16.
135 J. Liu, E. Sheina, T. Kowalewski and R. D. McCullough, *Angew. Chem. Int. Ed.*, 2002, **41**, 329–332.
136 J. L. Thelen, A. A. Teran, X. Wang, B. A. Garetz, I. Nakamura, Z.-G. Wang and N. P. Balsara, *Macromolecules*, 2014, **47**, 2666–2673.
137 I. Nakamura, N. P. Balsara and Z.-G. Wang, *ACS Macro Lett.*, 2013, **2**, 478–481.
138 S. N. Patel, A. E. Javier and N. P. Balsara, *ACS Nano*, 2013, **7**, 6056–6068.
139 M. P. Bhatt, J. L. Thelen and N. P. Balsara, *Chem. Mater.*, 2015, **27**, 5141–5148.
140 H. Wang, H. H. Wang, V. S. Urban, K. C. Littrell, P. Thiyagarajan and L. Yu, *J. Am. Chem. Soc.*, 2000, **122**, 6855–6861.
141 W. Y. Huang, S. Matsuoka, T. K. Kwei, Y. Okamoto, X. Hu, M. H. Rafailovich and J. Sokolov, *Macromolecules*, 2001, **34**, 7809–7816.
142 M. J. Im, B. J. Moon, G.-Y. Lee, S. Y. Son and T. Park, *J. Polym. Sci. Part Polym. Chem.*, 2014, **52**, 1068–1074.
143 J. W. Thackeray, H. S. White and M. S. Wrighton, *J. Phys. Chem.*, 1985, **89**, 5133–5140.
144 V. Rani and K. S. V. Santhanam, *J. Solid State Electrochem.*, 1998, **2**, 99–101.
145 D. Ofer, L. Y. Park, R. R. Schrock and M. S. Wrighton, *Chem. Mater.*, 1991, **3**, 573–575.
146 D. Ofer, R. M. Crooks and M. S. Wrighton, *J. Am. Chem. Soc.*, 1990, **112**, 7869–7879.
147 E. W. Paul, A. J. Ricco and M. S. Wrighton, *J. Phys. Chem.*, 1985, **89**, 1441–1447.
148 H. S. White, G. P. Kittlesen and M. S. Wrighton, *J. Am. Chem. Soc.*, 1984, **106**, 5375–5377.
149 M. Nishizawa, T. Matsue and I. Uchida, *Anal. Chem.*, 1992, **64**, 2642–2644.
150 J. Stejskal, O. E. Bogomolova, N. V. Blinova, M. Trchová, I. Šeděnková, J. Prokeš and I. Sapurina, *Polym. Int.*, 2009, **58**, 872–879.
151 M. G. Minett and J. R. Owen, *Solid State Ion.*, 1988, **28–30**, 1192–1196.
152 J. Tarver, J. E. Yoo, T. J. Dennes, J. Schwartz and Y.-L. Loo, *Chem. Mater.*, 2009, **21**, 280–286.
153 F. Sugiyama, A. T. Kleinschmidt, L. V. Kayser, D. Rodriquez, M. Finn, M. A. Alkhadra, J. M.-H. Wan, J. Ramírez, A. S.-C. Chiang, S. E. Root, S. Savagatrup and D. J. Lipomi, *Polym. Chem.*, 2018, **9**, 4354–4363.
154 B. Meng, H. Song, X. Chen, Z. Xie, J. Liu and L. Wang, *Macromolecules*, 2015, **48**, 4357–4363.
155 E. E. Sheina, S. M. Khersonsky, E. G. Jones and R. D. McCullough, *Chem. Mater.*, 2005, **17**, 3317–3319.
156 A. Giovannitti, D.-T. Sbircea, S. Inal, C. B. Nielsen, E. Bandiello, D. A. Hanifi, M. Sessolo, G. G. Malliaras, I. McCulloch and J. Rivnay, *Proc. Natl. Acad. Sci.*, 2016, **113**, 12017–12022.
157 C. B. Nielsen, A. Giovannitti, D.-T. Sbircea, E. Bandiello, M. R. Niazi, D. A. Hanifi, M. Sessolo, A. Amassian, G. G. Malliaras, J. Rivnay and I. McCulloch, *J. Am. Chem. Soc.*, 2016, **138**, 10252–10259.
158 A. Giovannitti, C. B. Nielsen, D.-T. Sbircea, S. Inal, M. Donahue, M. R. Niazi, D. A. Hanifi, A. Amassian, G. G. Malliaras, J. Rivnay and I. McCulloch, *Nat. Commun.*, 2016, **7**, 13066.
159 Y. Liao, V. Strong, W. Chian, X. Wang, X.-G. Li and R. B. Kaner, *Macromolecules*, 2012, **45**, 1570–1579.
160 C. H. W. Cheng, F. Lin and M. C. Lonergan, *J. Phys. Chem. B*, 2005, **109**, 10168–10178.
161 A. Laiho, L. Herlogsson, R. Forchheimer, X. Crispin and M. Berggren, *Proc. Natl. Acad. Sci.*, 2011, **108**, 15069–15073.

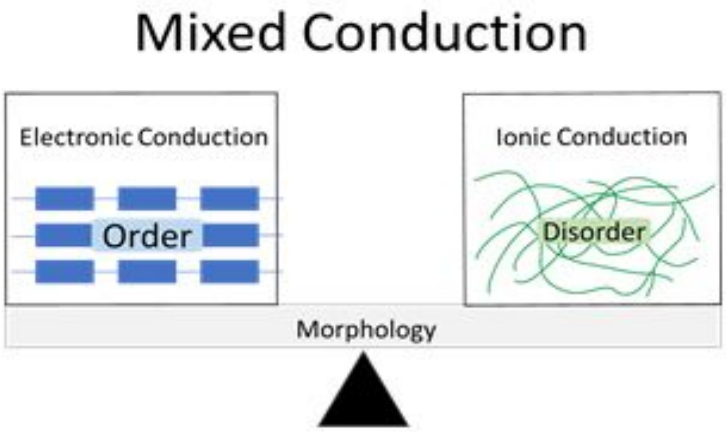

A review highlighting the implications of morphology on the mixed conduction performance of polymers.